Supporting Information

Safe and durable high-temperature lithium-sulfur batteries via molecular layer deposited coating

Xia Li,† Andrew Lushington,† Qian Sun,† Wei Xiao,†,⊥ Jian Liu,†,‡ Biqiong Wang,†,⊥ Yifan Ye,‡,# Kaiqi Nie,‡,∥ Yongfeng Hu,§ Qunfeng Xiao,§ Ruying Li,† Jinghua Guo,‡ Tsun-Kong Sham,⊥ and Xueliang Sun,†*

†Department of Mechanical and Materials Engineering, University of Western Ontario, ON, N6A 5B9, Canada ‡Advanced Light Source, Lawrence Berkeley National Laboratory, MS6R2100, One cyclotron road, Berkeley, CA, 94720, USA.

Corresponding Author: xsun9@uwo.ca.

Methods

Preparation of carbon-sulfur electrode: Commercial carbon black (KJ EC-600, US) was mixed with sulfur powder (99.5 %, Sigma-Aldrich) and dried at 80 ^{o}C for 12 h to remove moisture. The mixture was then transferred to a sealed steel reactor and was heated at 150 ^{o}C for 9 h and then 300 ^{o}C for 3 h. The obtained carbon-sulfur composites (C-S) maintained 65 wt% sulfur loading. The electrodes were prepared by slurry casting onto aluminum foil. The slurry mass ratio of active material, acetylene black, and polyvinylidene fluoride (PVDF) is 70:20:10. The as-prepared electrodes were finally dried at 80 ^{o}C over 12 h under vacuum.

Preparation of alucone coating on C-S electrode by MLD: Molecular layer deposition of alucone was conducted in a Gemstar-8 ALD system (Arradiance, USA). Alucone was directly

deposited on the C-S electrode at 100 ^{o}C by alternatively introducing trimethylaluminium (TMA) and ethylene glycol (EG). As studied from previous research, the growth rate of alucone thin film is < 0.3 nm/MLD cycle, and the sulfur loading of the C-S electrode dropped by 5 wt% after alucone coating.

Electrochemical characterization: CR-2032 type coin cells were assembled in an argon-filled glove box. The coin-type cells consisted of Li foil as the anode, polypropylene membrane (Celgard 2400) as separator, and the C-S electrode prepared above as the cathode. Two electrolyte systems were selected in this reserach: (1) carbonate-based electrolyte composed of 1 M $LiPF_6$ solution in ethylene carbonate:diethyl carbonate:ethyl methyl carbonate (EC:DEC:EMC) with a volume ratio of 1:1:1, and (2) ether-based electrolyte composed of 1 M LiTFSI salt in dioxolane (DOL): dimethoxyethane (DME) of 1:1 volume ratio. Cyclic voltammograms were collected on a versatile multichannel potentiostation 3/Z (VMP3) under a scanning rate of 0.1 mV s^{-1} between 1.0 V - 3.0 V (vs. Li/Li^{+}). Electrochemical impedance spectroscopy (EIS) was also performed on the versatile multichannel potentiostat 3/Z (VMP3) by applying an AC voltage of 5 mV amplitude in the 100 kHz to 100 mHz frequency range. All of batteries were tested by holding 6 hours after assembling. Charge-discharge characteristics were galvanostatically tested in the range of 1.0 V - 3.0 V (vs. Li/Li^{+}) at room temperature using an Arbin BT-2000 Battery Test equipment.

Physical characterization: The morphologies of the samples were characterized by Hitachi S-4800 field emission scanning electron microscope (FE-SEM) equipped with energy dispersive spectroscopy (EDS). Fourier transform-infrared (FTIR) measurements were determined by KBr method with a Nicolet 6700 FT-IR recorded in the transmittance mode over range of 400-4000 cm^{-1} spectra by averaging 40 scans with a resolution of 8 cm^{-1}. Thermogravimetric analysis (TGA) was carried out in a nitrogen atmosphere from room temperature to 600 °C at a heating rate of 10 °C/min on the SDT Q600 (TA Instruments). Syntrochron based near edge X-ray absorption fine structure (NEXAFS) and high energy X-ray photoelectron spectra

(HEXPS) measurements were carried out under two separate beamlines. Sulfur K-edge X-ray NEXAFS spectra were collected in total electron yield (TEY) mode on beamline 10.3.2 in the Advanced Light Source at Lawrence Berkeley Nathional Laboratory. Sulfur 1s HEXPS spectra was conducted on the Soft X-ray Microcharacterization beamline (SXRBM) with different values of photo energy at the Canadian Light Source (CLS) at the University of Saskatchewan in Saskatoon. Before synchrotron radiation experiments, original C-S electrodes and after battery test ones were preapred under protected environment. To avoid oxydation of samples, the C-S electrodes after discharge-charge processes were obtained from coin cells and sealed in glovebox under Argon, and then transferred to the corresponding beamlines for further measurements.

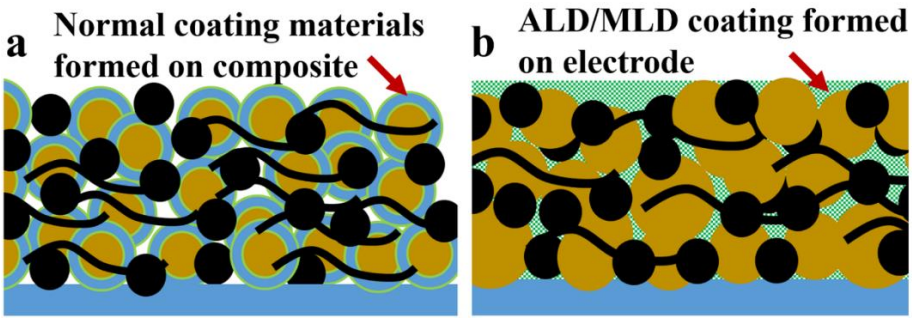

Scheme S1. Comparison of (a) normal coating materials and (b) ALD/MLD coating for sulfur cathodes.

Different from normal coating deposited on composites, MLD and ALD processes enable a conformal coating thin film growth on as-prepared electrodes, which demonstrates the generality of MLD and ALD technology applied in sulfur cathodes and other electrode materials.

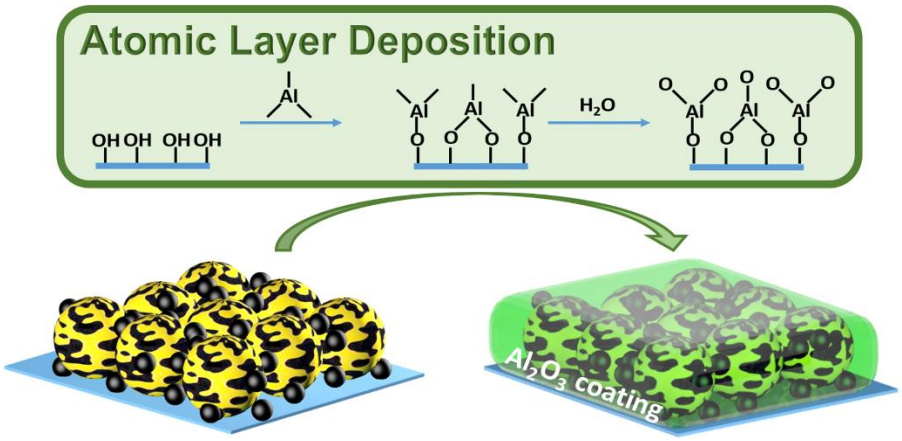

Scheme S2. Atomic layer deposition process on C-S electrodes.

Table S1. Physical properties of different electrolyte systems[1-3]

	Conventional Li-ion battery electrolyte (carbonate-based)			**Conventional Li-S battery electrolyte (ether-based)**	
Li Salt	Lithium hexafluorophosphate ($LiPF_6$)			Bis(trifluoromethane)sulfonimide lithium (LiTFSI)	
Additive	No			$LiNO_3$	
Solvents	Ethylene carbonate (EC)	Diethyl carbonate (DEC)	Ethyl methyl carbonate (EMC)	1,3-dioxolane (DOL)	1,2-dimethoxyethane (DME)
Boiling Point (ºC)	244-245	126-128	107	74-75	84-85
Flash Point (ºC)	160	31	26.7	< -1	< -2
Auto ignition Point (ºC)	465	445	440	273	200
**Data are given for materials in their standard state (at 25 °C [77 °F], 100 kPa.)*					

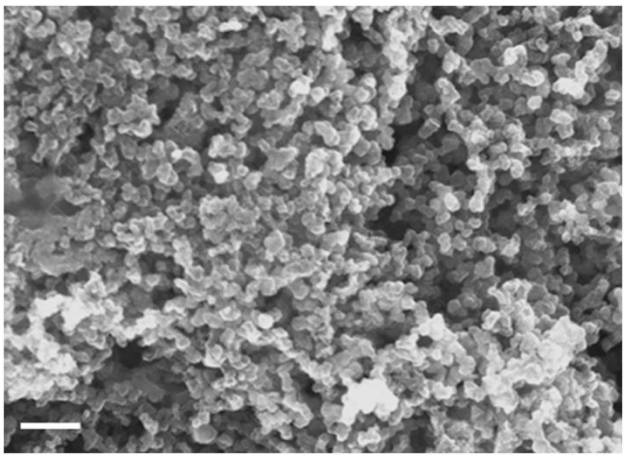

Figure S1. FE-SEM image of carbon-sulfur electrode with scale bar 200 nm.

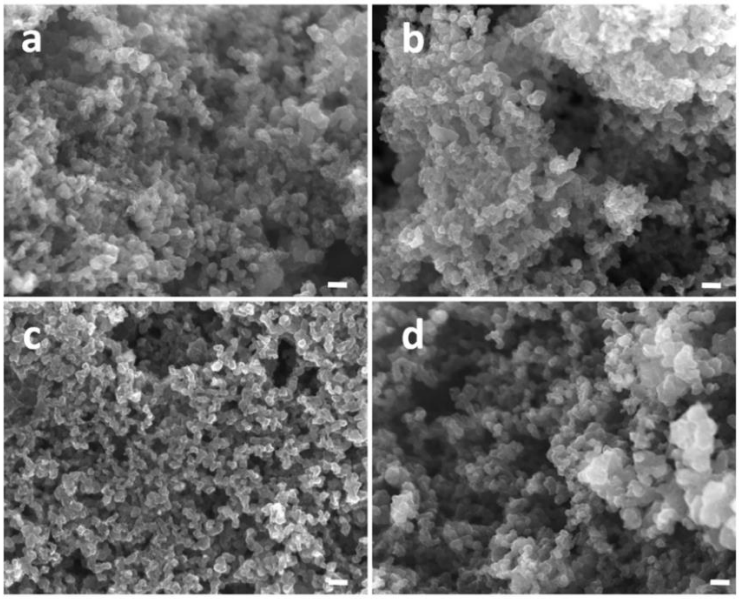

Figure S2. FE-SEM images of C-S electrodes (scale bar 100 nm) with different MLD cycles of alucone coating (a) 2-cycle, (b) 5-cycle, (c) 10-cycle, and (d) 20-cycle. Scale bar 100 nm (a-d).

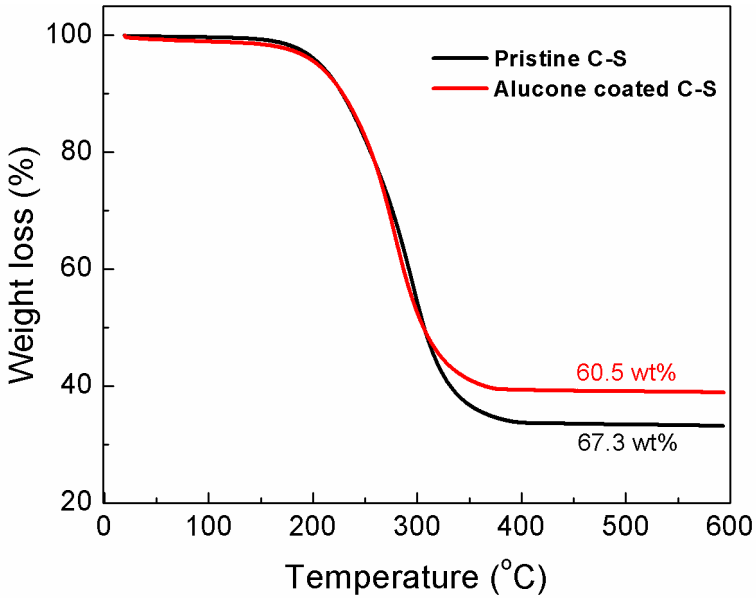

Figure S3. TGA profiles of as-prepared C-S composites.

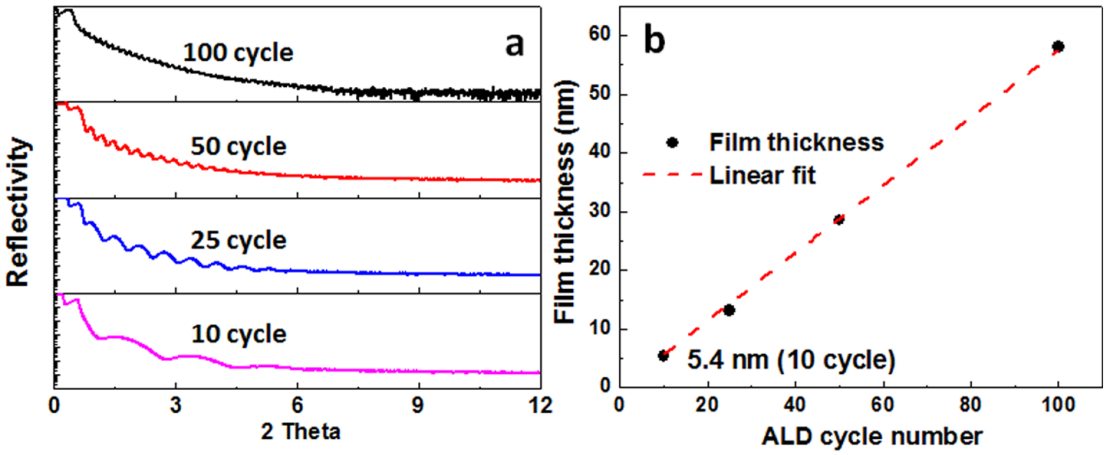

Figure S4. (a) XRR spectra of alucone thin film with different MLD cycles on silicon film substrates, and (b) linearity of alucone thin film thickness vs. MLD cycle.

As shown in Figure S4b, the thickness of 10, 25, 50, and 100-cycle MLD alucone films were obtained by X-ray reflectivity measurement, demonstrating linear growth of alucone thin films on silicon substrate. The thickness of 10-cycle alucone coating is around 5.4 nm with a growth rate of around 0.57 nm/ MLD cycle

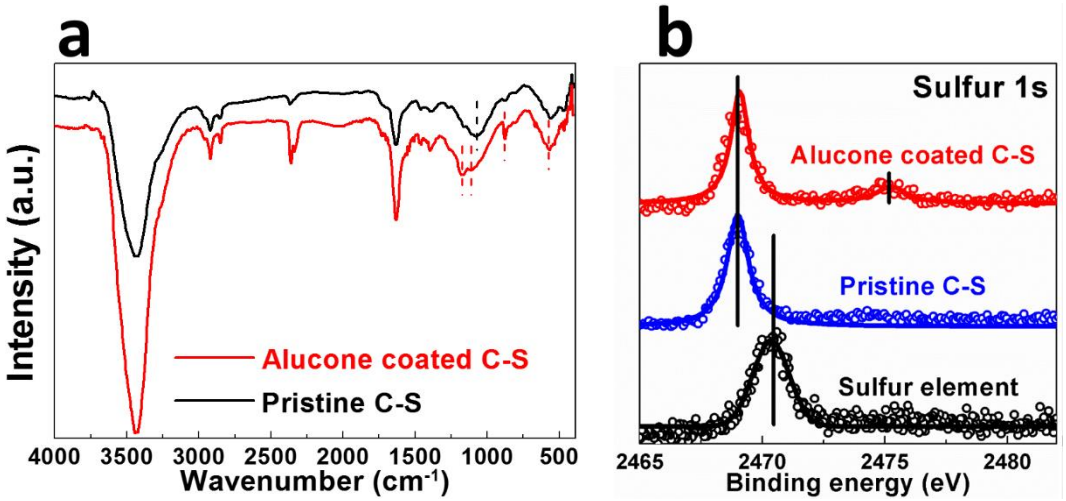

Figure S5. (a) FTIR specrta and (b) sulfur 1s HEXPS spectra of alucone coated and pristine C-S electrodes.

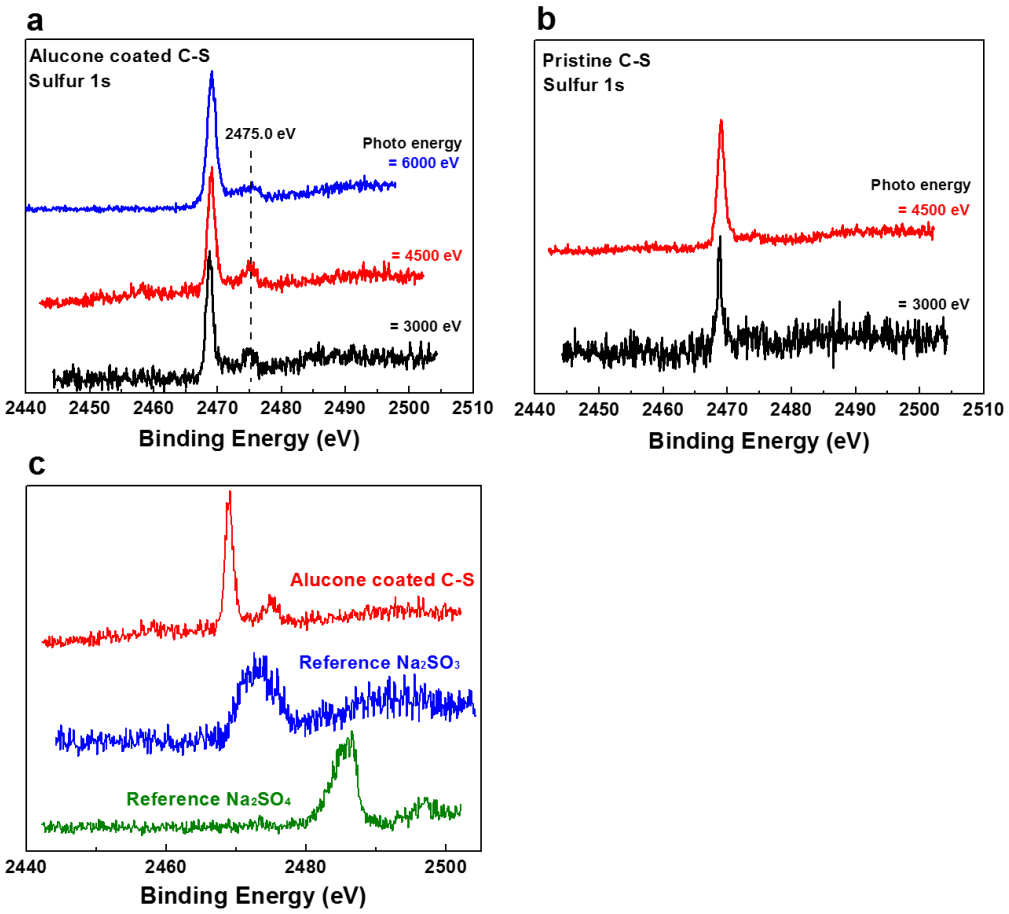

Figure S6. Sulfur 1s HEXPS spectra of (a) alucone coated C-S electrode, (b) pristine C-S electrodes, and (c) comparison of alucone coated C-S electrode and references.

SXRMB beamline at CLS enables tunable photo energy in HEXPS measurement. The employed photo energy reflects the probing depth to samples, which allows us to obtain informations from surface to bulk of sample. The three of photo energies we chose (3000 eV, 4500 eV, and 6000 eV) are able to detect different depth of sample, which are 3-5 nm, 5-7 nm, and 7-10 nm respectively. As shown in Figure S6a, the intensity of peaks at 2475.0 eV varies from different photo energies in sulfur 1s spectra. The peak shows the highest intensity with 4500 eV of photo energy (probing depth around 5-7 nm), while at 6000 eV (probing depth 7-10 nm) the peak turns weak. It demonstrates that very few sulfur on the surface of electrode (around 5 nm) interacts with alucone coating after MLD process. We believe that the chemical interaction between sulfur and alucone coating is related to the electrochemical reaction, which passivates the surface of sulfur cathode and enables reversible electrochemical reaction in carbonate electrolyte for sulfur cathodes. In this stage, the chemical state of the few interacted sulfur and detailed molecular structure of the interaction are still unclear. According to the comparison with chemical references shown in Figure S6c, we predict that the oxidation state of sulfur from surface may be between SO_3^{2-} and SO_4^{2-}. Detailed research will be carried out to further understand by synchrotron-based in-situ batteries characterizations in future.

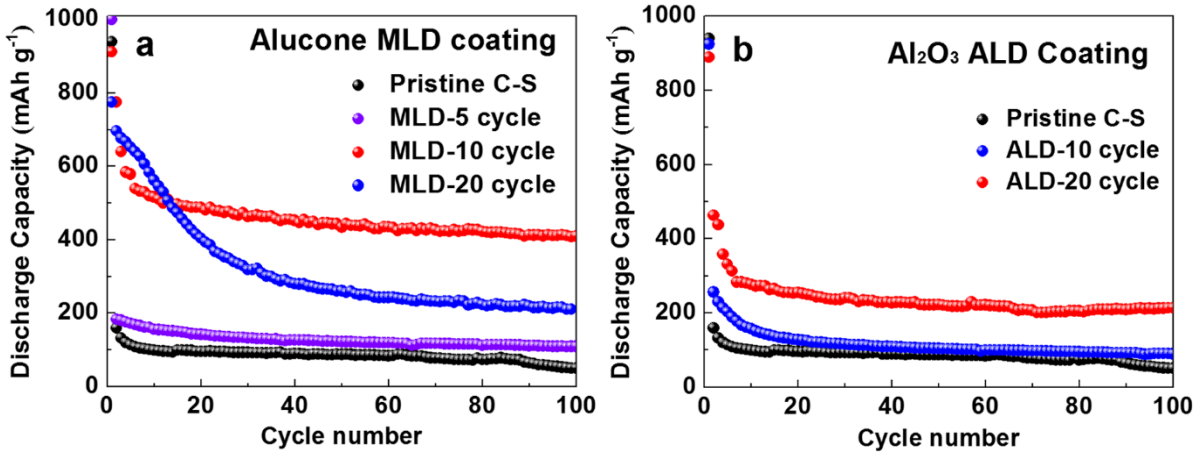

Figure S7. Thickness effect of MLD alucone and ALD Al_2O_3 coating.

The thickness of coating directly effects on the performance of Li-S batteries in carbonate-based electrolyte. As shown in Figure S7, 5-cycle MLD coating and 10-cycle ALD coating still cannot help to realize a convertional electrochemical performance of batteries, which exhibit very low discharge capacities from the second cycle. With the cycle number increasing, MLD (10-cycle) and ALD (20-cycle) coating demonstrate their support on sulfur cathode, which shows drastical improvement in cycle performance. It indicates that the coating layer should be thick enough or covering enough for C-S electrodes. Further increasing the thickness of coating layer (MLD coating 20-cycle) will bring higher interfacial resistence in Li-S batteries which demonstrates a reversible but lower discharge capacity in cycle. Another interesting phonomenon is that the cycle performance from MLD coating is better than that of ALD coating, which we propose alucone coating layer may facilitate Li-ion diffusion than Al_2O_3 coating. The mechanisms of MLD and ALD coating need further investigation and more measurements to demonstrate in future.

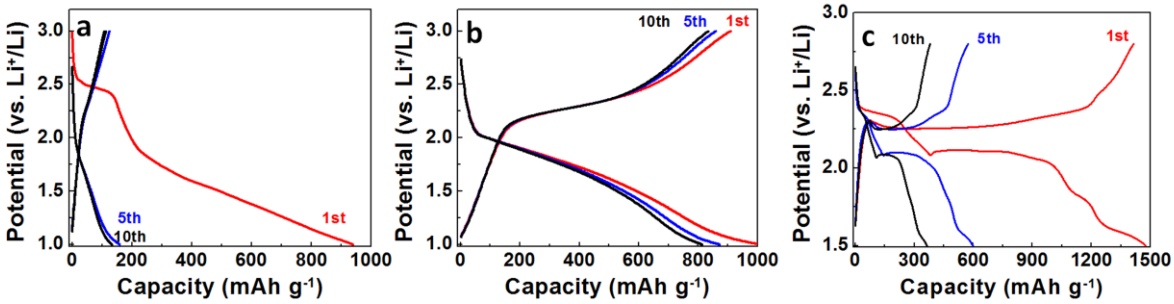

Figure S8. Discharge-charge curves of (a) pristine C-S electrode in carbonate based electrolyte at room tempreature; (b) alucone coated C-S electrode in carbonate based electrolyte; and (c) alucone coated C-S electrode in ether based electrolyte at high temperature.

A typical sulfur cathode in ether based electrolyte undergoes a two-step discharge process with Li metal, as shown in Figure S8c, corresponding to solid sulfur transferring to dissolved long-chain polysulfides (2.3 V, solid to liquid phase), followed by long-chain polysulfides further reducing to multiple short-chain sulfides (2.1 V, liquid to solid phase). However, the sulfur cathode in carbonate based electrolyte demonstrate an alternative electrochemical process. As shown in Figure S8a, due to the side-reaction of polysulfides and carbonate solvents, pristine C-S electrode are unable to complete a reversible Li-S electrochemical reaction. The alucone coated C-S electrode, on the other hand, undergoes a reversible electrochemical reaction with Li anode via an all-solid-phase process, which is only one potential plateau shown during discharge process.

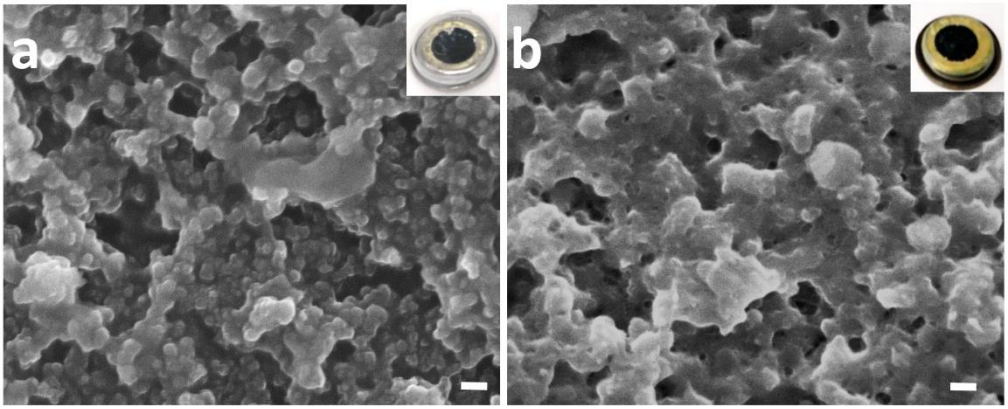

Figure S9. FE-SEM images of alucone coated C-S electrodes after electrochemical test under 55 ^{o}C (a) in carbonate based electrolyte; (b) in ether based electrolyte.

From images, it can be observed the electrolyte and seperator turned yellow with the use of ether based electrolyte. The surface of electrode is also deposited a thick layer of discharge product, as shown in FE-SEM image. Nevertheless, the electrode operating in carbonate electrolyte maintain transparent liquid electrolyte and fewer discharge product deposition on the surface, demonstrating a stable cycling process of Li-S batteries with carbonate electrolyte running at high temperature.

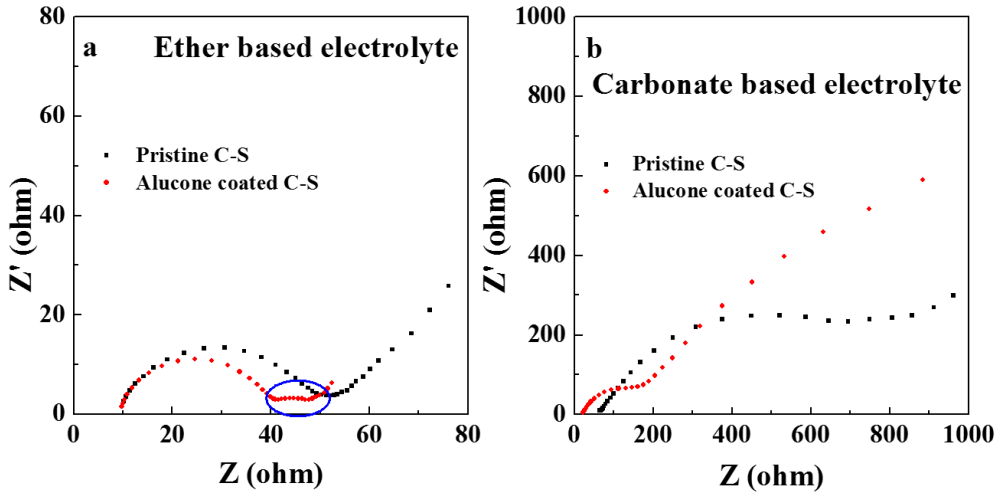

Figure S10. EIS profiles of C-S electrodes in different electrolytes.

To gain insight toward the influence of the MLD coating on the conductivity of the electrode, electrochemical impedance spectra (EIS) was carried out. As shown in Figure S10a, the spectra of both pristine and alucone coated C-S electrodes consist of a semi-circle in the high frequency region and a straight line in the low frequency region. Both alucone coated and pristine electrodes display a small semicircle, indicating that the electrode with MLD coating maintains small surface charge-transfer resistance and high electrochemical activity. However, the alucone coating electrode also displays a short line between the semicircle and straight line (as indicated by the blue circle), which indicates an extra-interlayer existing as a result of the MLD coating and may be attributed to increased resistance toward Li-ion diffusion. Figure S10b shows the EIS profiles of electrodes in carbonate based electrolyte. Interestingly, the surface charge-transfer resistance of MLD coated electrodes is much smaller compared to pristine electrodes. Corresponding to electrochemical performance, the alucone coating can protect sulfur from side reaction with carbonate solvents and maintain high activity toward electrochemical reactions. The pristine C-S electrode may form a thick layer on the surface due to the side reactions, thereby making reversible Li-S reaction cycling unfavorable.

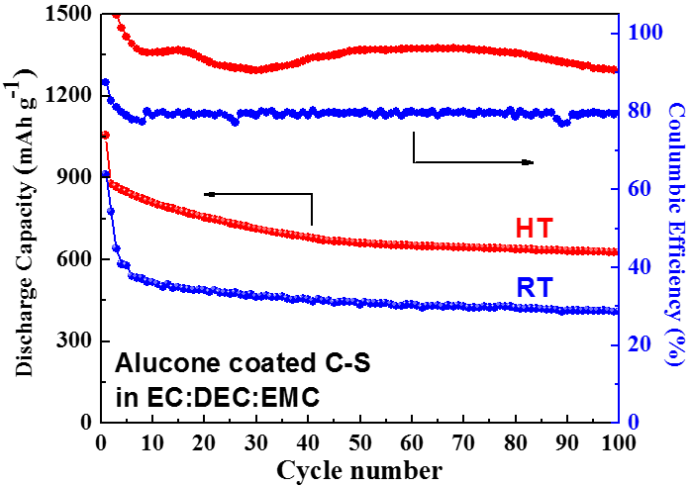

Figure S11. Alucone coated C-S electrode under room and high temperature.

The coulombic efficiency of alucone coated C-S electrode, is only around 80 % and 90 % at room and elevated temperature, respectively. The elevated temperature promote the evaporation of electrolyte and therefore cause the fluctuation of the Coulombic efficiency during cycling at high temperature.[4-6] This unsatisfactory performance is predominately influenced by two factors. One is the carbonate electrolyte itself, which may be related to Li anode deposition and will be further optimized via employing additive in carbonate electrolyte to improve the performance.[7, 8] The second is the carbon host and coating material employed, which will undoubtedly influence performance of Li-S batteries. The carbon host we employed in this report is commercial mesoporous carbon and the conductivity of the alucone MLD coating is quite limited. We aim to develop a highly conductive MLD coating with advanced carbon host to further improve the performance of high temperature Li-S batteries.

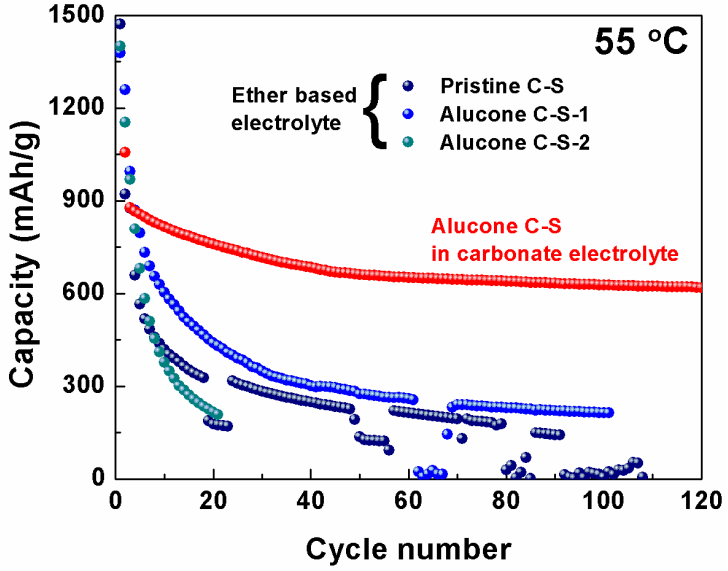

Figure S12. Cycle performance of electrodes in different electrolytes at high temperature.

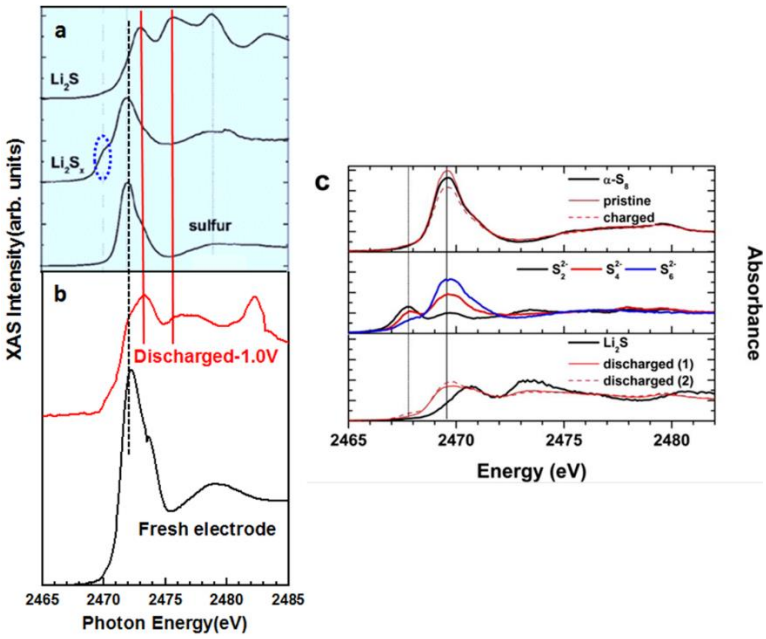

Figure S13. XANES spectra of (a, c) references samples[9, 10] and (b) alucone coated C-S electrode at different electrochemical stages.

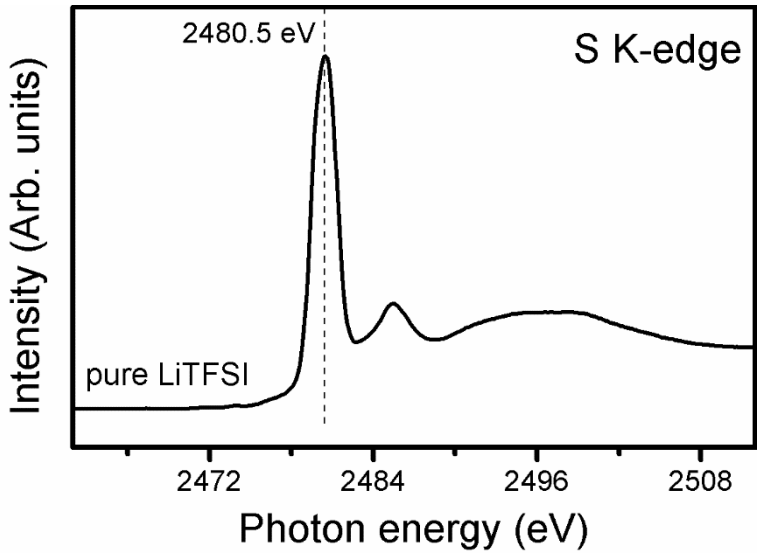

Figure S14. Sulfur K-edge spectrum of LiTFSI salt.

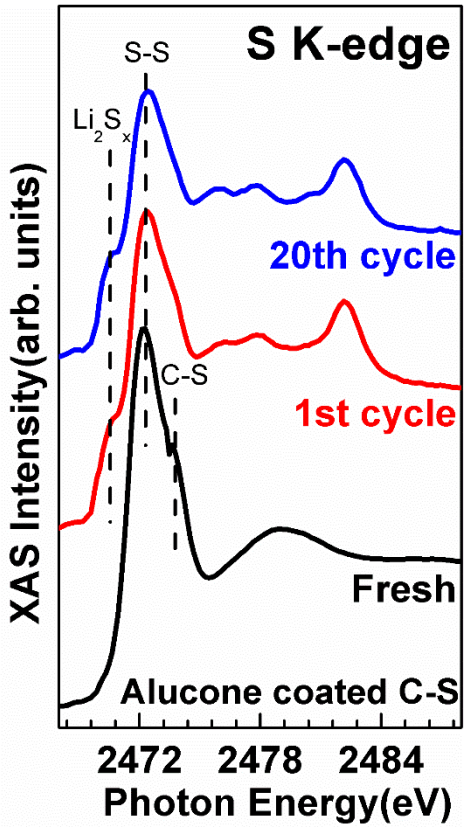

Figure S15. Sulfur K-edge spectra of alucone coated C-S electrodes after discharge-charge cycles.

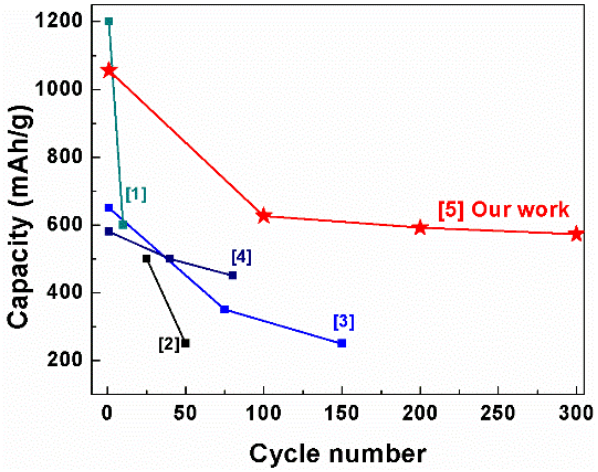

Figure S16. Comparison of references with our work from Table S2.

Table S2. Summary of literature results and our work in high temperature Li-S batteires.

	Cycle performance (Discharge capacity)	**Temperature**	**Electrolyte**	**Sulfur load**	**Reference**
1.	Around 650 mAh g^{-1}/10th cycle at 0.1 C (only test 10 cycles)	45 ^{o}C	LiTFSI (DOL:DME:BTFE) Additive: $LiNO_3$	70 wt%	*ACS applied materials & interfaces*, 2014, **6**, 8006-8010
2.	Less than 250 mAh g^{-1}/50th cycles at 0.1 C	45 ^{o}C	LiTFSI (DOL:DME) Additive: $LiNO_3$	68 -75 wt%	*J Power Sources*, 2014, **259**, 289-299
3.	Less than 250 mAh g^{-1}/150th cycles at 2 C	70 ^{o}C	LiTFSI (DOL:DME) Additive: $LiNO_3$	1.75 mg cm^{-2}	*J Power Sources*, 2013, **226**, 256-265.
4.	Less than 450 mAh g^{-1}/80th cycles at 1 C	60 ^{o}C	LiTFSI (DOL:DME)	66 wt%	*Nano Energy*, 2013, **2**, 314-321
5.	**570 mAh g^{-1}/300th cycle at 0.1 C**	55 ^{o}C	$LiPF_6$ (EC:DEC:EMC)	65 wt%	***Our work***

References

(1) Haynes, W. M., ed. CRC Handbook of Chemistry and Physics, 96th Edition; CRC Press/Taylor and Francis, Boca Raton, FL, 2016.
(2) National Institute of Standards and Technology. Http://webbook.nist.gov/ (February, 2016).
(3) National center for biotechnology information. Http://www.ncbi.nlm.nih.gov/ (November, 2015).
(4) Leng, F.; Tan, C. M.; Pecht, M. Sci. Rep. 2015, 5, 12967.
(5) Shi, J. Y.; Yi, C.-W.; Kim, K. J. Power Sources 2010, 195, 6860-6866.
(6) Hu, Q.; Osswald, S.; Daniel, R.; Zhu, Y.; Wesel, S.; Ortiz, L.; Sadoway, D. R. J. Power Sources 2011, 196, 5604-5610.
(7) Etacheri, V.; Haik, O.; Goffer, Y.; Roberts, G. A.; Stefan, I. C.; Fasching, R.; Aurbach, D. Langmuir 2012, 28, 965-76.
(8) Aurbach, D.; Gamolsky, K.; Markovsky, B.; Gofer, Y.; Schmidt, M.; Heider, U. Electrochim. Acta 2002, 47, 1423-1439
(9) Patel, M. U.; Arcon, I.; Aquilanti, G.; Stievano, L.; Mali, G.; Dominko, R. Chemphyschem 2014, 15, 894-904.
(10) Cuisinier, M.; Cabelguen, P.-E.; Evers, S.; He, G.; Kolbeck, M.; Garsuch, A.; Bolin, T.; Balasubramanian, M.; Nazar, L. F. J. Phys. Chem. Lett. 2013, 4, 3227-3232.